Biosensors and Bioelectronics 58 (2014) 351–358

Contents lists available at ScienceDirect

Biosensors and Bioelectronics

journal homepage: www.elsevier.com/locate/bios

Carbon nanodots–chitosan composite film: A platform for protein immobilization, direct electrochemistry and bioelectrocatalysis

Meili Sheng [a,b,c], Yue Gao [a,b,c], Junyong Sun [a,b,c], Feng Gao [a,b,c,*]

[a] Laboratory of Functionalized Molecular Solids, Ministry of Education, College of Chemistry and Materials Science, Anhui Normal University, Wuhu 241000, PR China
[b] Anhui Key Laboratory of Chemo/Biosensing, College of Chemistry and Materials Science, Anhui Normal University, Wuhu 241000, PR China
[c] Laboratory of Optical Probes and Bioelectrocatalysis (LOPAB), College of Chemistry and Materials Science, Anhui Normal University, Wuhu 241000, PR China

ARTICLE INFO

Article history:
Received 19 November 2013
Received in revised form
20 February 2014
Accepted 3 March 2014
Available online 12 March 2014

Keywords:
Carbon nanodots
Hemoglobin
Bioelectrocatalysis
Direct electron transfer
Biosensor
Hydrogen peroxide

ABSTRACT

A novel composite film based on carbon nanodots (CNDs) and chitosan was readily prepared and used as immobilization matrix to entrap a heme protein, hemoglobin (Hb) for direct electrochemistry and bioelectrocatalysis. A modified electrode was obtained by casting Hb–CNDs–chitosan composites on the glassy carbon (GC) electrode surface. Spectroscopic and electrochemical studies showed that Hb entrapped in the composite film remained in its native structures, and CNDs in the film can greatly facilitate DET between the protein and the GC electrode. The electron-transfer kinetics of Hb in composite film was qualitatively evaluated by using the Marcus theory, and the apparent heterogeneous electron-transfer rate constant (k_s) was estimated to be 2.39($\pm$0.03) s^{-1} with Laviron equations. The modified electrode showed excellent electrocatalytic behavior to the substrate, hydrogen peroxide (H_2O_2). The linear current response for H_2O_2 was from 1×10^{-6} to 1.18×10^{-4} M with a detection limit of 0.27($\pm$0.02) μM at the signal-to-noise ratio of 3, and the apparent Michaelis–Menten constant was 0.067($\pm$0.02) mM. These important features of CNDs–chitosan film have implied to be a promising platform for elaborating bioelectrochemical devices such as biosensors and biofuel cells.

1. Introduction

Direct electron transfer (DET) between native redox-active proteins and electrodes has become a popular topic among the studies on electron transfer reactions of redox proteins since the two pioneered reports on DET between cytochrome *c* and gold electrode by Hill (Eddowes and Hill, 1977), and cytochrome *c* and tin doped indium oxides electrode by Kuwana (Yeh and Kuwana, 1977) in 1977. Studies on DET process of redox protein–electrode system are of scientific importance not only in investigating the fundamental mechanism of protein-mediated biological redox reactions such as photosynthesis, respiration and bioenergetic metabolism Voet and Voet (1993), but also in fabricating mediator-free (without redox relays) bioelectrochemical devices such as biosensors, bioreactors and biofuel cells (Flexer et al., 2011; Gao et al., 2007; Gao et al., 2011a, 2011b). However, it is generally difficult to achieve DET between redox proteins and conventional bare electrodes due to some obstacles including unfavorable orientation of protein moleculars on electrode surface, long distance between redox-active centers and electrode, adsorption denaturation of protein moleculars on electrode surface (Léger and Bertrand, 2008), and electrode passivation resulting from the adsorption of the large three-dimensional structure of protein moleculars on electrode surface (Stellwagen, 1978). Hb is probably one of the most extensively studied proteins for DET investigations and DET-based bioelectrochemical applications. However, the facilitation of DET between the heme-centers within the large three-dimensional structure and the electrode is still a challenge.

Fortunately, favorable electrode materials and stable protein immobilization could provide an opportunity to facilitate DET process of redox proteins. Thus, it is very intriguing to modify conventional electrodes with favorable materials and immobilization method to entrap proteins on electrode surface to achieve DET process, and consequently fabricate practical bioelectrochemical devices. Over the past decades, the modification of the electrode surface with varied nanomaterials composed of metal oxides (Si et al., 2011;Yang et al., 2012), and conducting polymers (Wang et al., 2009) has appeared to facilitate DET between proteins and the electrode because the unique chemical, physical, and electrical properties of nanostructured materials may

* Corresponding author at: Laboratory of Functionalized Molecular Solids, Ministry of Education, College of Chemistry and Materials Science, Anhui Normal University, Wuhu 241000, PR China. Tel.: +86 553 3937136; fax: +86 553 3869302.
E-mail address: fgao@mail.ahnu.edu.cn (F. Gao).

http://dx.doi.org/10.1016/j.bios.2014.03.005
0956-5663/

effectively shorten the electron-tunneling distance and provide an electron-mediating function. A wide variety of carbon-based nanomaterials, such as carbon nanotubes, carbon nanofibers, carbon nanochips, and graphene oxide, have shown to be ideal electrode materials and the capabilities of DET since they possess high conductivity, good biocompatibility, ease of functionalization, and large surface area (George and Lee, 2009; Gooding et al., 2003; Kumar et al., 2012; Lu et al., 2008; Shan et al., 2009; Vamvakaki et al., 2006; Wang, 2005; Wu et al., 2007; Zuo et al., 2010).

CNDs are very interesting newcomers to the world of carbonaceous nanomaterials and constitute a fascinating class of nanocarbons that comprise discrete, quasi-spherical nanoparticles with sizes below 10 nm Baker and Baker (2010). Owing to their important photoluminescent properties dependent on size and wavelength, lack of any known cytotoxicity, resistance to photobleaching, CNDs are emerging as viable alternatives to traditional semiconductor-based quantum dots, and fascinating luminescent materials as well as promising building blocks for future nanodevices (Yang et al., 2012). Currently, the immense research interests in CNDs are primarily driven by their excellent photoluminescent properties and have shown their potential applications in a broad range of areas such as optical sensing, bioimaging, and light energy conversion Baker and Baker (2010). However, similar to their popular older cousins including fullerenes, carbon nanotubes, and graphene, CNDs also possess several favorable attributes of carbon-based nanomaterials as described in foregoing paragraph. These remarkable characteristics make CNDs suitable for the supports of biocatalysts and electrochemical signal transduction. However, utilization of CNDs in this area has not been reported so far. Such limited attention is not proportional to the remarkable properties and potential merits of CNDs.

Different approaches, such as covalent attachment, adsorption, electrostatic interactions, and film entrapment have been used to immobilize proteins on the electrode surface (Lojou and Bianco, 2004). Among these approaches, film entrapment is of greater interest because the ultrathin films can probably provide a suitable microenvironment for proteins to retain their native structures and enhance DET between the proteins and electrodes. To attain this, substances with film-forming ability, such as SiO_2, Nafion, room-temperature ionic liquids are generally used to form films to entrap proteins. Chitosan, a natural polysaccharide biopolymer derived from chitin, is composed of β(1→4) linked glucosamine units together with some proportion of N-acetylglucosamine units. It is an attractive linear hydrophilic biopolymer that exhibits excellent biologic compatibility and film-forming ability (Peniche et al., 2003). Owing to its relatively poor conductivity, chitosan was usually combined with conducting materials such as carbon materials, redox mediators, metal nanoparticles, and ionic liquid to form conductive film for entrapping proteins (Lu et al., 2006; Zhang et al., 2004).

In this study, a composite film formed with chitosan and CNDs is considered as an excellent immobilization matrix for Hb entrapment, as shown in Scheme 1. The homogeneous solution containing chitosan, CNDs, and Hb can be readily made into film on GC electrode surface after it is dried. CNDs embedded in the three-dimensional chitosan network can serve as conductor due to its good intrinsic conductivity, and Hb–CNDs–chitosan composite film modified electrode (defined as Hb–CNDs–chitosan/GC) can be prepared by a very simple approach. Ultraviolet visible (UV–vis) and Fourier transform infrared (FT-IR) spectroscopy were used to identify the morphological and structural variations of Hb immobilized in the CNDs–chitosan film. Direct electrochemistry and bioelectrocatalysis of Hb toward H_2O_2 reduction were demonstrated at Hb–CNDs–chitosan/GC electrode, and thereafter a third-generation (without redox mediators) biosensor for H_2O_2 was established.

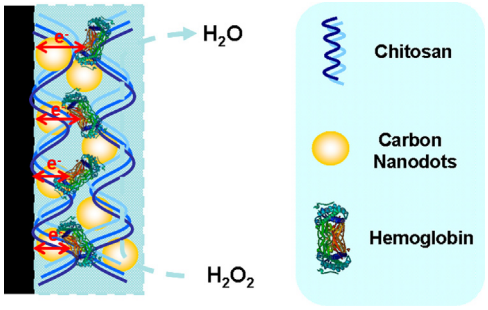

Scheme 1. Schematic illustration of Hb–CNDs–chitosan system.

2. Experimental

2.1. Materials and chemicals

Hb (from Bovine blood, MW=67,000) was purchased from Sigma. Chitosan (from crab shells, minimum 90% deacetylated), hydrogen peroxide (H_2O_2, 30% w/w), and other chemicals were all obtained from Sinopharm Chemicals Co., Ltd. (Shanghai, China). All the chemicals were of at least analytical grade and used without further purification. All solutions were prepared with Milli-Q purified water (> 18.0 MΩ).

A 50 mM pH 7.4 phosphate buffer solution (PBS) prepared by 50 mM Na_2HPO_4 and 50 mM KH_2PO_4 solution was used as supporting electrolyte. The dilute H_2O_2 solution was prepared freshly and only used daily. A 1.0 mg mL^{-1} stock Hb solution was prepared by dissolving 1 mg Hb in 1.0 mL PBS. Chitosan aqueous solution was prepared according to the previously reported protocols (Zhang et al., 2004) and is shown in Supplementary data. CNDs were prepared with candle soot as starting material according to reported methods (Li et al., 2011; Zhang et al., 2013) and is also shown in Supplementary data. The CNDs were dispersed into chitosan solution to give a homogeneous suspension with the aid of ultrasonic agitation. The mixture solution for Hb entrapment was prepared by adding an appropriate volume of chitosan solution, Hb solution, and CNDs into PBS. To obtain good cyclic voltammetric responses, a typical mixture solution containing 0.15 mg mL^{-1} chitosan, 0.25 mg mL^{-1} hemoglobin, and 0.40 mg mL^{-1} CNDs was used for preparing modified electrodes.

2.2. Apparatus

All the electrochemical experiments were carried out on CHI660C potentiostat (CHI, Shanghai) with a conventional three-electrode cell. A modified electrode was used as the working electrode, a Ag/AgCl as the reference electrode, and a platinum wire as the counter electrode. The experimental solutions were bubbled with highly pure nitrogen for 30 min to deoxygenate and kept under nitrogen atmosphere during the electrochemical measurements. The electrochemical measurements were performed at room temperature and repeated minimum three times. UV–vis absorption spectra were measured on UV-3010 spectrophotometer (Hitachi, Japan), and FT-IR 8400S spectrophotometer (Shimadu, Japan) was used for IR spectra using KBr pellet samples.

2.3. Electrode preparation

Prior to use, GC electrode (⌀=3 mm) was pretreated with conventional method. A 4 μL of resultant mixture solution for Hb entrapment was cast onto the electrode surface by using a 10-μL micro-syringe to prepare an Hb–CNDs–chitosan/GC electrode. A beaker was covered over the electrode so that solvent can be evaporated slowly in air and a uniform film can be formed. The

dried Hb–CNDs–chitosan/GC electrode was stored at 4 °C in a refrigerator when not in use. The resulting electrodes were rinsed with water before use. For comparison, Hb/GC and Hb–chitosan/GC electrodes with the same loading of Hb and chitosan were prepared with the same procedures as described above.

3. Results and discussion

3.1. General characterization

Fig. 1A shows the typical SEM image of CNDs and it is clear that the CNDs are uniform in size. From the SEM image of Hb–CNDs–chitosan/GC depicted in Fig. 1B, we can see that the CNDs are discernible, and all of the constituents of the modified electrode agglomerated to form film-like structures. In this composite, CNDs were embedded in the chitosan to form a stable composite film, which is essential for the stability of the prepared electrode. The CNDs entrapped in the three-dimensional chitosan network can serve as conductor due to its good intrinsic conductivity. Furthermore, CNDs can dramatically enhance the active surface area of the modified GC electrode available for Hb entrapment compared to bare GC electrode. Fig. 1C (from left to right side) presents the photos of Hb–CNDs, Hb–CNDs–chitosan, and Hb–CNDs–chitosan composite kept for one week, respectively. We can see that a homogeneous solution can be readily obtained and also can be kept for a longer time without precipitation upon chitosan, Hb, and CNDs are mixed together. The composites can provide a friendly microenvironment for Hb to retain its good bioactivity, and also provide a favorable platform for Hb to realize DET.

It is important to examine conformational variation of Hb entrapped in CNDs–chitosan film. Spectroscopic methods such as UV–vis and FT-IR spectroscopy are generally employed for comparing the structural variations of native and immobilized Hb (George and Lee, 2009). UV–vis spectroscopy is a useful tool for conformational studies of heme proteins and can provide information for different conformational states of Hb, which is because the position of the Soret absorption band (B band) of heme may also provide information on possible denaturation of heme protein, particularly on conformational change in the heme group region (Rusling and Nassar, 1993). Fig. 2A shows the UV–vis spectra of native Hb (curve *a*) and the composite Hb–CNDs–chitosan (curve *b*) in PBS, respectively. It is clearly that the characteristic Soret band of Hb in Hb–CNDs–chitosan film did not show obvious alteration and appeared at almost the same position as the native Hb solution at 405 nm, indicating that Hb essentially retained its native conformation in the presence of CNDs and chitosan. FT-IR spectroscopy is usually used to provide detailed information on the secondary structure of polypeptide chains and detect conformational changes of proteins. The shape and position of amide I (1700–1600 cm^{-1}) and amide II (1600–1500 cm^{-1}) bands provide detailed information on the secondary structure of the polypeptide chain (Kauppinen et al., 1981). The amide I band at 1700–1600 cm^{-1} is attributed to C═O stretching vibrations of the peptide linkage, and the amide II band at 1600–1500 cm^{-1} results from a combination of N–H in-plane bending and C–N stretching of the peptide groups. As shown in Fig. 2B, the spectra of the amide I (1655 cm^{-1}) and II (1543 cm^{-1}) bands of Hb in the Hb–CNDs–chitosan film (curve *b*) were almost as same as those of native Hb (1653 and 1543 cm^{-1}, curve *a*). The FT-IR also demonstrated that Hb in Hb–CNDs–chitosan film retained the essential features of its native structure.

To investigate the stability of Hb–CNDs–chitosan film by UV–vis spectroscopy, a certain amount of Hb–CNDs–chitosan mixed solution was cast on a clean glass sheet, and the spectra of dry Hb–CNDs–chitosan/glass sheet immersed in PBS for different time were collected (Fig. S1). The results showed that no obvious changes of absorption spectra and peak intensities were observed after 24 h, suggesting that Hb in Hb–CNDs–chitosan film would not diffuse into buffer solution and Hb was efficiently immobilized into the composite film. We contribute these distinguished characteristics to both the good biocompatibility of the composite system and the strong interaction between Hb and CNDs–chitosan film.

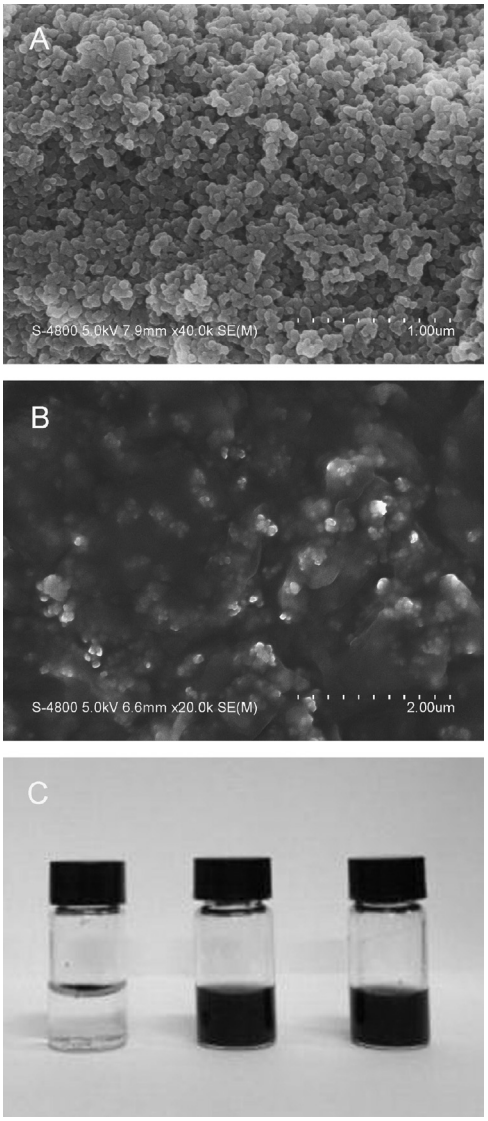

Fig. 1. SEM images of CNDs (A), Hb–CNDs–chitosan/GC (B), and the photos of Hb–CNDs, Hb–CNDs–chitosan, and Hb–CNDs–chitosan composite kept for one week (C), from left to right side.

3.2. Electrochemical characterization and measurements

3.2.1. Electrochemical impedence characterization of modified electrodes

The electrochemical impedance spectroscopy (EIS) was employed to monitor the processes of electrode fabrication. The electron transfer resistance of the electrochemical reaction, R_{ct}, which corresponds to the semicircle diameter of the Nyquist plot of $-Z''$ against Z', reveals the electron transfer kinetics of the redox electrochemical probe at the electrode interface. The EIS spectra of the bare GC, Hb/GC, Hb–chitosan/GC, and Hb–CNDs–chitosan/GC

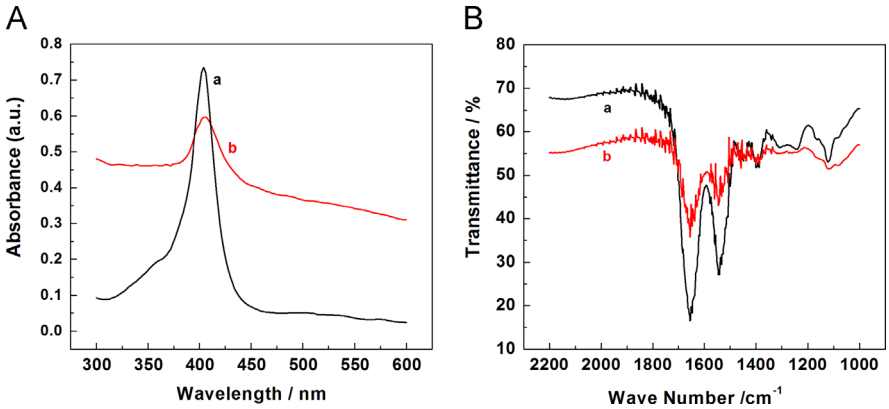

Fig. 2. UV–vis spectra (A) and FT-IR spectra (B) of native Hb (curve *a*), and Hb in Hb–CNDs–chitosan composite (curve *b*).

electrodes were recorded in 5 mM $[Fe(CN)_6]^{3-/4-}$ solution containing 0.1 M KCl and shown in Fig. S2. The bare GC electrode showed an almost straight line (curve *a*), which is characteristic of a diffusion-limited step of the electrochemical process. After Hb was confined on the GC electrode, the resulting Hb/GC electrode showed a larger semicircle, corresponding to the larger electron transfer resistance (curve *b*). This is because the electronic repulsion between negatively charged Hb (Hb in pH 7.4 PBS has considerable negative charges because the isoelectric point of Hb is at 7.0–7.4) and the probing moleculars. As shown in Fig. S2, the diameter of the semicircular part for the Hb–CNDs–chitosan/GC electrode (curve *c*) is much smaller than that of Hb–chitosan/GC electrode (curve *d*), indicating that the charge-transfer resistance of the Hb–CNDs–chitosan/GC electrode is decreased upon the introduction of CNDs into the Hb–chitosan film. This result confirms that the presence of CNDs in the film plays an important role in enhancing electron transfer and makes it easier to take place, thus decreasing the resistance of the Hb–CNDs–chitosan film to probing moleculars.

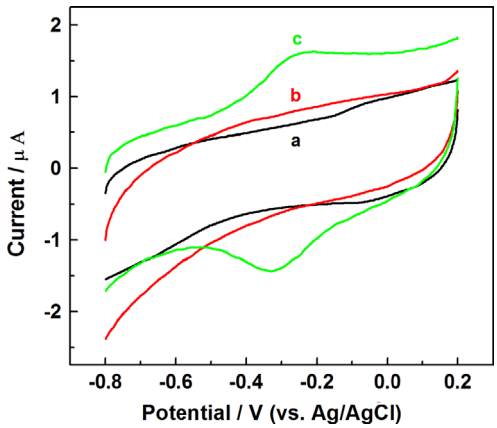

Fig. 3. CVs of Hb/GC (curve *a*), Hb–chitosan/GC (curve *b*), and Hb–CNDs–chitosan/GC (curve *c*) electrodes recorded in deoxygenated pH 7.4 PBS with a scan rate of 500 mV s^{-1}.

3.2.2. *Direct electrochemistry of Hb immobilized in CNDs–chitosan film*

The DET behaviors of Hb on different modified electrodes were investigated by cyclic voltammetry. Fig. 3 shows the cyclic voltammograms (CVs) of Hb/GC (curve *a*), Hb–chitosan/GC (curve *b*) and Hb–CNDs–chitosan/GC (curve *c*) electrodes recorded in deoxygenated PBS with a scan rate of 500 mV s^{-1}. At the Hb–CNDs–chitosan/GC electrode, a pair of well-defined and nearly symmetric redox peaks was observed, which could be ascribed to the electron transfer between Hb and the underlying electrode. The cathodic peak potential (E_{pc}) and anodic peak potential (E_{pa}) are −0.328 V and −0.250 V (vs. Ag/AgCl), respectively. The formal potential, $E^{0'}$ (defined as the average of E_{pa} and E_{pc}) is −0.289 V, which is consistent with the reported values for the Fe^{III}/Fe^{II} redox center of the heme group in Hb (Gao et al., 2011b; Wang, 2005). Furthermore, the peak-to-peak separation, ΔE_p (defined as $\Delta E_p = E_{pa} - E_{pc}$) is ca. 78 mV and the ratio of anodic peak current (I_{pa}) and cathodic peak current (I_{pc}), I_{pa}/I_{pc}, was approximately 1, indicating that Hb immobilized in the CNDs–chitosan film displayed a one-electron quasi-reversible redox electrochemical reaction. No obvious redox peaks were observed at the Hb/GC or Hb–chitosan/GC electrode, which is possibly due to the unfavorable orientation or denaturing of Hb molecules on the bare GC electrode surface, or the poor conductivity of chitosan that hinders DET between Hb and the GC electrode. Comparing with the Hb/GC or Hb–chitosan/GC electrodes, Hb–CNDs–chitosan/GC electrode can provide a conductive microenvironment that facilitates the electron transfer between the Hb and the GC electrode due to the entrapment of CNDs in the film. In order to obtain good cyclic voltammetric responses at the Hb–CNDs–chitosan/GC electrode, the loading and the mass ratios of Hb, chitosan, and CNDs in Hb–chitosan–CNDs were optimized in control experiments (Supplementary data). The experimental results demonstrated that a total loading of ca. 3.2 μg and the concentration ratios for Hb, chitosan, and CNDs (in mg mL^{-1}) in Hb–CNDs–chitosan composite film of 0.25, 0.15, and 0.40, respectively, are optimal.

For the Hb–CNDs–chitosan/GC electrode, the peak current reached steady state after several CV cycles in buffer. Thus, all of the CV experiments at the Hb–CNDs–chitosan/GC electrode were conducted at their steady states. The CVs of Hb–CNDs–chitosan/GC electrode in deoxygenated PBS with different scan rates from 40 to 2000 mV s^{-1} were collected. As shown in Fig. S3A, the anodic and cathodic peak potentials show little changes and currents for the DET reaction of Hb are linear with the increasing of scan rates (Fig. S3B), indicating that all of the electroactive Hb–Fe^{III} in the film was reduced to Hb–Fe^{II} on the forward scan and then reoxidized to Hb–Fe^{III} on the reverse scan. Substantially, the charge consumed in coulombs (Q) calculated from integrating the anodic or cathodic peak area in the CVs under the background correction was invariable. Furthermore, $I_{pc} - \nu$ and $I_{pa} - \nu$ plots were linear and the ratio of the slopes (S_{Ipc}/S_{Ipa}) was close to 1 (Fig. S3B). These results demonstrate that Hb immobilized in CNDs–chitosan film undergoes a quasi-reversible and surface-controlled thin-layer electrochemical process (Rusling and Nassar, 1993; Zhou et al., 2002).

The average surface concentration of electroactive Hb (Γ^*, mol cm^{-2}) can be estimated from the charge integration of the

oxidation peak of the CV using the following formula:

$$\Gamma^* = Q/nFA$$

where Γ^* is the amount of electroactive species, Q represents the average reacted electric quantity (C, coulombs), n is the number of transfer electrons ($n=1$), F is the Faraday constant, and A is the geometric area of the GC electrode (0.0707 cm^2). According to this method and assuming a single electron transfer reaction, the amount of electroactive Hb molecules at the Hb–CNDs–chitosan/GC electrode was estimated to be 8.78×10^{-11} mol cm^{-2}, which is almost as 4.6 times as that of the theoretical monolayer coverage (1.89×10^{-11} mol cm^{-2}) (Wang et al., 2005). This result suggests that several layers of Hb entrapped in the composite film participated in the electron-transfer process. The absolute surface concentration of Hb cast on the geometric area of the electrode was estimated to be 2.11×10^{-10} mol cm^{-2}. Thus, the fraction of electroactive Hb was calculated to be 41.6%, which is about 1.5 times higher than that of the reported value of Hb entrapped in Nafion–carbon nanofiber composite film (Lu et al., 2008). This high fraction of electroactive Hb in Hb–CNDs–chitosan film is possibly attributed to the following facts: (1) CNDs–chitosan film provides ideal platforms for the favorable orientation of Hb molecules to retain their bioactivity; (2) the high surface area of CNDs can dramatically enhance the active surface area of the GC electrode available for protein entrapment; (3) CNDs may act as nanoscaled conductive electrical wires, just like other carbon-nanomaterials including carbon nanotubes, carbon nanofibers, and carbon nanochip, to facilitate the DET between proteins and the underlying electrode; (4) the combination of CNDs with chitosan helps proteins to be readily entrapped within the composites because of the good film-forming ability of the composites; (5) the organic–inorganic hybrid may provide better biocompatibility and stability along with higher bioactivity for the immobilization of proteins.

The interfacial electron transfer rate (k_s) at the Hb–CNDs–chitosan/GC electrode can be estimated using the equation derived by Laviron (Laviron, 1979; Laviron and Roullier, 1980).

$$\log\ k_s = \alpha\log(1-\alpha)+(1-\alpha)\log\ \alpha-\ \log\left(\frac{RT}{nFv}\right)-\alpha(1-\alpha)\frac{nF\Delta E_p}{2.3RT}$$

The symbols R, T, and F have their usual meanings, n is the electron transfer number for Hb. Since the peak-to-peak separation (ΔE_p) was less than 200/n mV (Fig. S3A), the electron transfer coefficient α is taken as 0.5. The average kinetic electron transfer rate constant k_s is estimated to be 2.39 ($\pm$0.03) s^{-1}, which is larger than the value of 1.984 s^{-1} with gold colloid-solk fibroin modified electrode (Guo et al., 2009), 1.90 s^{-1} with Hb/mesoTiO$_2$ modified electrode (Chen and Lu, 2006), and 0.90 s^{-1} with polymer–Hb–MWNTs modified electrode (Jia et al., 2008), indicating that the electron transfer rate of Hb entrapped in the Hb–CNDs–chitosan film is fast. We attribute this enhanced electron transfer to the distinguished characters of Hb–CNDs–chitosan film described above.

The electron-transfer kinetics of Hb in composite film was also qualitatively evaluated by using the Marcus theory (Marcus and Sutin, 1985). The protein DET is usually assumed to take place within the non-adiabatic electron-transfer regime because the protein matrix provides a weak electronic coupling between the electrode and the enzyme prosthetic group (Moser and Dutton, 1996). Based on the semiclassical model of Marcus equation, the rate constant for non-adiabatic electron transfer between weakly coupled donor and acceptor sites at a fixed distance depends on the driving force and the reorganization energy, λ (eV), required to change the nuclear co-ordinates of the donor to those of the acceptor without transferring the electron. Since electron transfer occurs to or from any Fermi level in the electrode, we combine the standard Marcus equation for non-adiabatic electron transfer with the Fermi–Dirac distribution for a dimensionless potential difference from the applied potential E (i.e., the Fermi level). The total electron-transfer rate constant at a given E is obtained by summing the contribution of all states, as previously reported and expressed as following Chidsey (1991), Hirst and Armstrong (1998), Mazzei et al. (2008). The electron-transfer rate constant ($k_{red/ox}$) increases with the energy difference, reaches a maximum value (k_{max}) and then decreases again at higher driving force (the inverted region). The pre-exponential factor k_{max} depends on the electronic coupling between the donor and the acceptor.

$$k_{red/ox} = k_{\max}\sqrt{\frac{RT}{4\pi\lambda}}\int_{\infty}^{-\infty}\frac{\exp\left(-\frac{\lambda\pm F(E-E^{o'})}{RT}-x\right)^2\frac{RT}{4\lambda}}{\exp(x)+1}dx$$

As shown in Fig. S4A and B, an increase in reduction and oxidation peak separation as well as in half-height peak width ($W_{1/2}$) was observed at increasing scan rates, indicating both trends are in agreement with the Marcus model.

3.2.3. Influence of solution pH on the DET of Hb

The influence of pH on the electrochemical behavior of Hb in the Hb–CNDs–chitosan/GC electrode was also studied. Fig. S5A displays the features of CVs of Hb–CNDs–chitosan/GC electrode in electrolytic solution with different pH values ranging from 5.0 to 9.0. As shown in Fig. S5A, the CVs with stable and well-defined peaks were observed, and the CVs showed a strong dependence on pH of the solution. However, both the oxidation and reduction peak potentials in voltammograms shifted negatively with the increase of pH. The formal potential ($E^{\circ\prime}$) showed linearly response to the solution pH (Fig. S5B), suggesting the redox reaction was companied with proton transfer. The slope for $E^{\circ\prime}$–pH plot was estimated to be about −45.3 mV/pH with the correlation coefficient of 0.9974, which is reasonably close to the expected value calculated for the one-proton transfer coupled one-electron-transfer reaction using the Nernst equation at 25 °C (Bard and Faulkner, 2001), and also in agreement with the reported values (Gao et al., 2011b; Guo et al., 2009). We have to note that the slope value is smaller than the theoretical value, which may attribute to the influence of the protonation of trans and residue ligands around the heme and the protonation of the water molecules coordinated with the central iron (Yamazaki et al., 1978). This indicate that the proton diffusion in electron transfer reaction is fast, and also confirm single proton (H^+) and single electron (e^-) participate in the electron transfer process of Hb. The electron process can be described as following:

$$\text{Hb heme } (Fe^{III}) + H^+ + e^- = \text{Hb heme } (Fe^{II})$$

All changes in voltametric peak potentials and currents with pH were reversible, that is, the same voltamogram can be obtained if the electrode is transferred from a solution with a different pH value back to its original solution.

3.3. H_2O_2 biosensor based on DET of Hb

3.3.1. Electrocatalytic activity of Hb–CNDs–chitosan/GC electrode to H_2O_2 reduction

As one kind of heme proteins, bioactive Hb immobilized on an electrode surface usually has good electrocatalytic activity for oxygen, TCA, NO_2^-, H_2O_2, etc. (Huang et al., 2002). In the present study, we studied the electrocatalytic properties of the Hb–CNDs–chitosan/GC electrode to H_2O_2 reduction as an example because the determination of H_2O_2 is of great importance in many fields, such as in clinical, food, pharmaceutical and environmental analysis.

The electrocatalytic activity to the reduction H_2O_2 by the Hb–CNDs–chitosan/GC electrode was investigated and characterized by cyclic voltammetry in deoxygenated PBS at a scan rate of 200 mV s^{-1}. As shown in Fig. 4, in the absence of H_2O_2, a pair of quasi-reversible and well-defined redox peaks was observed due to the DET reaction between entrapped Hb and electrode. Once the addition of H_2O_2, a significant increase in the reduction peak at about −0.30 V was observed, while the oxidation peak current was decreased simultaneously. The more amount of H_2O_2 was added, the greater the decrease in the oxidation peak, and the greater the increase in the reduction peak. Moreover, the reduction current increased gradually with the increasing of H_2O_2 concentration. However, no corresponding electrochemical signal could be observed in the same potential window using a CNDs–chitosan/GC electrode in the presence of H_2O_2 solution as shown in the inset of Fig. 4, indicating that the catalytic process came from the specific enzymatic catalytic reaction between Hb and H_2O_2. We also found that the anodic peak wave decreased and disappeared after the addition of a limiting concentration of H_2O_2 into the buffer solution. Such saturation behavior is the characteristic of an enzymatic catalysis. The mechanism can be expressed as follows (Gao et al., 2011b):

$$\text{Hb Heme } (Fe^{III}) + H^+ + e^- = \text{Hb Heme } (Fe^{II})$$

$$2\text{Hb Heme } (Fe^{II}) + H_2O_2 \rightarrow 2\text{Hb Heme } (Fe^{III}) + 2H_2O$$

From this expression, we can describe that Hb-Heme (Fe^{II}) generated on the electrode was chemically oxidized by H_2O_2, and the produced Hb-Heme (Fe^{III}) was reduced again at the electrode in a catalytic cycle. When increasing the H_2O_2 concentration, more and more Hb-Heme (Fe^{II}) was chemically oxidized, resulting in an increase of the Hb-Heme (Fe^{III}) reduction peak and a decrease of the Hb-Heme (Fe^{II}) oxidation peak.

Fig. 5A displays the amperometric responses of Hb–CNDs–chitosan/GC electrode to H_2O_2 with successive additions of H_2O_2 at an applied potential of −0.30 V to a continuous stirring deoxygenated buffer solution. Upon the addition of H_2O_2, the electrode responded rapidly to the substrate. The reduction current increased steeply within about 5 s to reach a stable value and the reduction current increased linearly with H_2O_2 concentration. The response time for amperometric measurements was much shorter than those reported about heme protein-based H_2O_2 biosensors (Feng et al., 2005; Lei and Deng, 1996; Pandey et al., 2001; Wang and Dong, 2000;

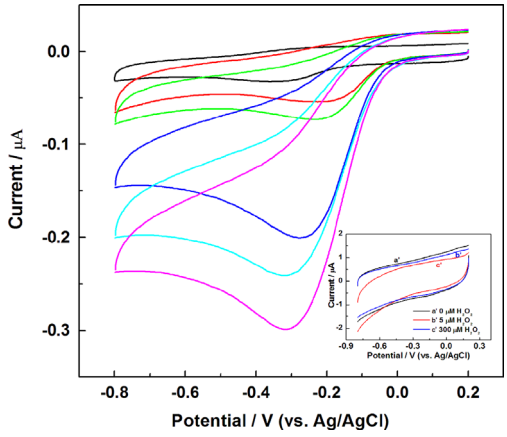

Fig. 4. CVs of Hb–CNDs–chitosan/GC electrode in 5 pH 7.4 PBS containing H_2O_2 (from inner to outer): 0.0 μM, 5 μM, 10 μM, 100 μM, 200 μM, 300 μM. Inset: cyclic voltammograms of CNDs–chitosan/GC electrode in 50 mM deoxygenated PBS (pH 7.4) in the presence of different concentrations of H_2O_2.

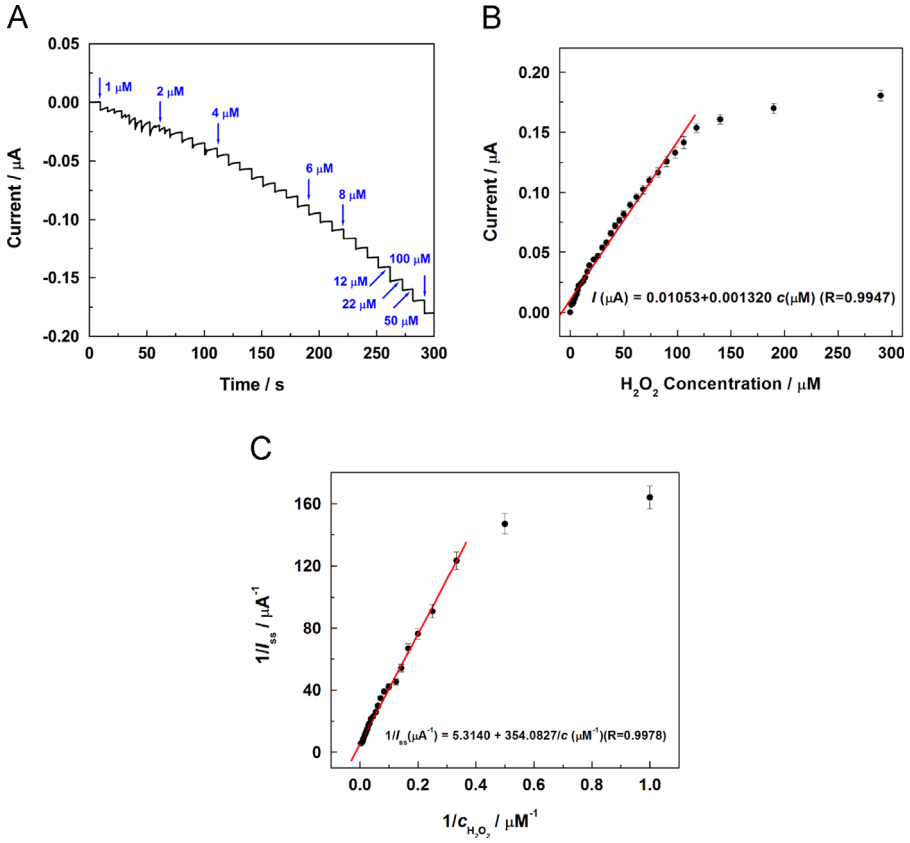

Fig. 5. (A) Amperometric responses of Hb–CNDs–chitosan/GC electrode upon successive additions of H_2O_2 in deoxygenated pH 7.4 PBS at −0.30 V. (B) The corresponding calibration plot of currents against H_2O_2 concentrations. Each data point represents the average value of five independent experiments with error bars indicated, and the relative standard deviation is 3.4%. (C) The plot of $1/I_{ss}$ against $1/c$. Error bars represent the range calculated using three different electrodes.

Zheng et al., 2008). The calibration curve for H_2O_2 detection is shown in Fig. 5B and a linear response ranges from 1×10^{-6} to 1.18×10^{-4} M with a correlation coefficient of 0.9947 ($n=33$) was obtained. The detection limit was estimated to be 0.27($\pm$0.02) μM at a signal-to-noise ratio of 3. The sensitivity of the electrode was found to be 1320 nA/mM. The comparative results of some analytical parameters for different H_2O_2 sensors are listed in Table S1. As shown in Table S1, the analytical parameters for the present H_2O_2 biosensor are comparable or better than the results reported for different H_2O_2 sensors.

As shown in Fig. 5B, when the concentration of H_2O_2 increases gradually, a response plateau is observed, showing the typical characteristics of Michaelis–Menten kinetic mechanism. The apparent Michaelis–Menten constant (K_M^{app}) is a characteristic of the film on the electrode, not of the enzyme, and usually differs substantially from the enzyme constant, measured in a homogenous solution. The apparent Michaelis–Menten constant can be obtained from the electrochemical version of Lineweaver–Burk equation (Cai and Chen, 2004; Fan et al., 2001; Sun et al., 2007).

$$\frac{1}{I_{ss}}=\frac{1}{I_{max}}+\frac{K_M^{app}}{I_{max}c}$$

here I_{ss} is the steady-state current after the addition of substrate, which can be obtained from the amperometric experiments, I_{max} is the maximum current under saturated substrate condition and c is the bulk concentration of the substrate. From the slope of the plot of $1/I_{ss}$ against $1/c$ as shown in Fig. 5C, the apparent Michaelis–Menten constant was calculated to be 0.067($\pm$0.02) mM. This value is much smaller than that reported for Hb entrapped in Nafion/nano-$CaCO_3$/ionic liquid of 0.12 mM (Sun et al., 2007), the Hb immobilized onto the surface of carbon nanotube of 41 mM (Cai and Chen, 2004), Hb entrapped SP dephadex membrane of 1.9 mM (Fan et al., 2001), and Hb immobilized on Au–Zrp of 0.65 mM (Feng et al., 2005). The low value of the apparent Michaelis–Menten constant indicates that Hb entrapped into the CNDs–chitosan film retains its higher bioactivity and has a much better affinity to H_2O_2.

3.3.2. Stability and reproducibility of the H_2O_2 biosensor

The storage stability of the electrode was investigated by monitoring its response to 50 μM H_2O_2. A ca. 4.1% decrease of initial current was observed after the storage of two weeks. The operational stability of the electrode was also examined by successive assays of 50 μM H_2O_2 using one same Hb–CNDs–chitosan/GC electrode. The electrode was regenerated by immersing in pH 7.4 PBS after each of the measurements. The reproducible current with a R.S.D. value of 2.9% was obtained for 11 successive assays. The reproducibility between five Hb–CNDs–chitosan/GC electrodes fabricated independently with the same way was also investigated. The five electrodes were used for the measurements of 50 μM H_2O_2 and showed a satisfactory R.S.D. of 3.6%. The good stability and reproducibility may be attributed to the stable entrapment of Hb in CNDs–chitosan film.

3.3.3. Interference determination of foreign species

The effect of some potential interfering substances such as glucose, uric acid, ascorbic acid, some amino acids, and inorganic ions on H_2O_2 determination was investigated. For this purpose, we examined amperometric response for 5 μM H_2O_2 in a mixed solution in the presence of 5 mM interfering species. As shown in Table S2, the error made by each interference is not noticeable ($<\pm5\%$). The results indicate that the modified electrode has a good selectivity for sensing H_2O_2 and displays potential application for H_2O_2 determination in real samples. The high selectivity of the present biosensor is attributed to the fast direct electron transfer rate of Hb at the modified electrode.

3.3.4. Determination of H_2O_2 in real samples using Hb–CNDs–chitosan/GC electrode

H_2O_2 is the product of oxidative stress and metabolism and play important role in clinical analysis. The feasibility of the proposed H_2O_2 biosensor for practical application was investigated through analysis of urine samples collected from individuals. The H_2O_2 concentrations detected in the samples by the Hb–CNDs–chitosan/GC electrode ranged from 0.11 to 0.17 mM (Table S3). The results obtained using the proposed biosensor were compared with those obtained using the classical potassium permanganate titration method. The results are in good agreement with each other, revealing the good practicality of our method.

4. Conclusions

CNDs–chitosan matrix was successfully used for the immobilization of Hb on the electrode surface. The entrapped Hb in CNDs–chitosan film retains its structural intactness and high bioactivity, and shows good affinity to H_2O_2, indicating that CNDs can act as efficient electrical wiring the redox centers of proteins to the electrode. The present work demonstrates that the usage of CNDs–chitosan composite film as matrix for proteins/enzymes entrapment is an attractive alternative to other immobilization methods and the combination of CNDs and chitosan will bring new opportunities for designing novel bioelectrocatalytic systems to fabricate bioelectrochemical devices such as biosensors and biofuel cells.

Acknowledgments

We are grateful for the financial support from the National Natural Science Foundation of China (Grant no. 21175002), Program for New Century Excellent Talents in University(NCET-12-0599), Anhui Provincial Natural Science Foundation for Distinguished Youth (Grant no. 1108085J09), and the project sponsored by SRF for ROCS, SEM.

Appendix A. Supplementary information

Supplementary data associated with this article can be found in the online version at http://dx.doi.org/10.1016/j.bios.2014.03.005.

References

Baker, S.N., Baker, G.A., 2010. Angew. Chem. Int. Ed. 49, 6726–6744.
Bard, A.J., Faulkner, L.R., 2001. Electrochemical Methods: Fundamentals and Applications. John Wiley and Sons, NewYork.
Cai, C., Chen, C., 2004. Anal. Biochem. 325, 285–292.
Chen, L., Lu, G.J., 2006. Electroanal. Chem. 597, 51–59.
Chidsey, C.E.D., 1991. Science 251, 919–922.
Eddowes, E.J., Hill, H.A.O., 1977. J. Chem. Soc. Chem. Commun. 21, 771–772.
Fan, C.H., Wang, H.Y., Sun, S., Zhu, D.X., Wagner, G., Li, G.X., 2001. Anal. Chem. 73, 2850–2854.
Feng, J., Xu, J., Chen, H., 2005. J. Electroanal. Chem. 585, 44–50.
Flexer, V., Brun, N., Courjean, O., Backov, R., Mano, N., 2011. Energy Environ. Sci. 4, 2097–2106.
Gao, F., Guo, X., Yin, J., Zhao, D., Li, M., Wang, L., 2011a. RSC Adv. 1, 1301–1309.
Gao, F., Yao, Z., Huang, Q., Chen, X., Guo, X., Ye, Q., Wang, L., 2011b. Colloids Surf. B 82, 359–364.
Gao, F., Yan, Y., Su, L., Wang, L., Mao, L., 2007. Electrochem. Commun. 9, 989–996.
George, S., Lee, H.K., 2009. J. Phys. Chem. B 113, 15445–15454.
Gooding, J.J., Wibowo, R., Liu, J.Q., Yang, W.R., Losic, D., Orbons, S., Mearns, F.J., Shapter, J.G., Hibbert, D.B., 2003. J. Am. Chem. Soc. 125, 9006–9007.
Guo, H., Liu, D., Yu, X., Xia, X., 2009. Sens. Actuators B: Chem. 139, 598–603.
Huang, H., Hu, N.F., Zeng, Y.H., Zhou, G., 2002. Anal. Biochem. 308, 141–151.

Hirst, J., Armstrong, F.A., 1998. Anal. Chem. 70, 5062–5071.
Jia, N., Wen, Y., Yang, G., Lian, Q., Xu, C., Shen, H., 2008. Electrochem. Commun. 10, 774–777.
Kauppinen, J.K., Moffat, D.J., Mantsch, H.H., Cameron, D.G., 1981. Appl. Spectrosc. 35, 271–275.
Kumar, A.S., Gayathri, P., Barathi, P., Vijayaraghavan, R., 2012. J. Phys. Chem. C 116, 23692–23703.
Laviron, E.J., 1979. Electroanal. Chem. 101, 19–28.
Laviron, E., Roullier, L.J., 1980. Electroanal. Chem. 115, 65–70.
Léger, C., Bertrand, P., 2008. Chem. Rev. 108, 2379–2438.
Lei, C., Deng, J., 1996. Anal. Chem. 68, 3344–3349.
Li, H., Zhai, J., Sun, X., 2011. Langmuir 27, 4305–4308.
Lojou, E.A., Bianco, P., 2004. Electroanalysis 16, 1113–1121.
Lu, X., Zhou, J., Lu, W., Liu, Q., Li, J., 2008. Biosens. Bioelectron. 23, 1236–1243.
Lu, X., Hu, J., Yao, X., Wang, Z., Li, J., 2006. Biomacromolecules 7, 975–980.
Marcus, R.A., Sutin, N., 1985. Biochim. Biophys. Acta 811, 265–322.
Mazzei, F., Favero, G., Frasconi, M., Tata, A., Tuccitto, N., Licciardello, A., Pepi, F., 2008. Anal. Chem. 80, 5937–5944.
Moser, C.C., Dutton, P.L., 1996. In: Bendall, D.S. (Ed.), Protein Electron Transfer. Bios Scientific Publishers, Oxford, pp. 1–21.
Pandey, P., Upadhyay, S., Tiwari, I., Tripathi, V., 2001. Sens. Actuators B: Chem. 72, 224–232.
Peniche, C., Argiielles-Monal, W., Peniche, H., Acista, N., 2003. Macromol. Biosci. 3, 511–520.
Rusling, J.F., Nassar, A.E.F., 1993. J. Am. Chem. Soc. 115, 11891–11897.
Shan, C.S., Yang, H.F., Song, J.F., Han, D.X., Ivaska, A., Niu, L., 2009. Anal. Chem. 81, 2378–2382.
Si, P., Ding, S., Yuan, J., Lou, X.W., Kim, D.H., 2011. ACS Nano 5, 7617–7626.
Stellwagen, E., 1978. Nature 275, 73–74.
Sun, W., Gao, R., Jiao, K., 2007. J. Phys. Chem. B 111, 4560–4567.
Vamvakaki, V., Tsagaraki, K., Chaniotakis, N., 2006. Anal. Chem. 78, 5538–5542.
Voet, D., Voet, J.G., 1993. Biochemistry, 2nd ed. John Wiley & Sons, New York
Wang, B., Dong, S., 2000. Talanta 51, 565–572.
Wang, J., 2005. Electroanalysis 17, 7–14.
Wang, S.F., Chen, T., Zhang, Z.L., Shen, X.C., Lu, Z.X., Pang, D.W., Wong, K.Y., 2005. Langmuir 21, 9260–9266.
Wang, Z.Y., Liu, S.N., Wu, P., Cai, C.X., 2009. Anal. Chem. 81, 1638–1645.
Wu, S., Ju, H.X., Liu, Y., 2007. Adv. Funct. Mater. 17, 585–592.
Yamazaki, I., Araiso, T., Hayashi, Y., Yamada, H., Makino, R., 1978. Adv. Biophys. 11, 249–281.
Yang, C., Xu, C., Wang, X., 2012. Langmuir 28, 4580–4585.
Yeh, P., Kuwana, T., 1977. Chem. Lett. 6, 1145–1148.
Zhang, L., Cui, P., Zhang, B., Gao, F., 2013. Chem. – Eur. J. 19, 9242–9250.
Zhang, M., Smith, A., Gorski, W., 2004. Anal. Chem. 76, 5045–5050.
Zheng, W., Zheng, Y.F., Jin, K.W., Wang, N., 2008. Talanta 74, 1414–1419.
Zhou, Y., Hu, N., Zeng, Y., Rusling, J.F., 2002. Langmuir 18, 211–219.
Zuo, X., He, S., Li, D., Peng, C., Huang, Q., Song, S., Fan, C., 2010. Langmuir 26, 1936–1939.